HYDROGEN, FUEL CELL & ENERGY STORAGE

Feasibility of Fabricating a Defect-Free Nickel Composite Membrane Using the Organic-Inorganic Activation Technique

Mina Omidifar | Ali Akbar Babalou*

Nanostructure Material Research Center (NMRC), Sahand University of Technology, P.O. Box 51335-1996, Sahand New Town, Tabriz, Iran

* Corresponding author, Email: a.babaluo@sut.ac.ir

Article Information

Article Type
Research Article

Article History
Received: *13 Nov 2025*
Revised: *03 Feb 2026*
Accepted: *03 Mar 2026*
Published Online: *07 Mar 2026*

Keywords

Nickel composite membrane
Hydrogen purification
Organic-inorganic activation method
Electroless plating
Knudsen diffusion

Abstract

This study presents a novel fabrication method for metal/ceramic membranes, providing a cost-effective substitute for traditional, expensive Pd-based membranes. While nickel offers a promising replacement for Pd-based membranes, its effectiveness in H_2 separation depends on whether it can function independently or must be incorporated into Pd-based alloys to enhance performance and reduce fabrication costs. To investigate this, a homogeneous and thin (2 μm) nickel composite membrane was fabricated with the organic-inorganic activation (OIA) process in the electroless plating (ELP) technique for the first time. At 25 °C and a differential pressure of 400 kPa, the hydrogen flux of the membrane was measured at 3.26×10^{-2} mol m^{-2}s^{-1}, with a separation factor of 3 for H_2/N_2. The findings demonstrated that Knudsen diffusion was the prevailing mechanism for H_2 transport across the membrane.

Cite this article: Abdali, S., Yaghoubi, S. (2026). Feasibility of Fabricating a Defect-Free Nickel Composite Membrane Using the Organic-Inorganic Activation Technique. DOI: 10.22104/hfe.2025.7498.1350

 Publisher: Iranian Research Organization for Science and Technology (IROST)
DOI: 10.22104/hfe.2025.7498.1350

1 Introduction

Global energy demand has risen dramatically in recent years due to fast population growth and economic development [1–4]. This demand has primarily been supplied by the widespread consumption of fossil fuels, resulting in their rapid depletion [5–7]. Furthermore, dependence on fossil fuels has resulted in serious environmental issues, including global warming and climate change, caused mainly by greenhouse gas emissions [8–10]. Overcoming this challenge requires the advancement of renewable energy sources and the adoption of innovative technologies to replace traditional systems [11–13]. H_2 emerges as a viable solution due to its high energy density and environmentally friendly nature, making it a zero-emission energy carrier [14–17]. Therefore, maximizing the efficiency of H_2 energy usage necessitates enhancements in hydrogen production and purification performance [18–21].

H_2 separation and purification are carried out using three commercial technologies: cryogenic distillation, membrane separation, and pressure swing adsorption (PSA) [14, 22–24]. Among these, membrane-based separation has received much attention due to its key advantages, including mild operational conditions, small equipment design, and cost-effectiveness, making it a very promising technology for hydrogen separation and purification [5,14,23,25]. H_2-permeable membranes used in membrane separation technologies can be divided into three categories based on their transport mechanisms: atomic, ionic (proton), and molecular [5, 26]. Among these, membranes for atomic transport, commonly called dense metallic membranes, exhibit exceptional hydrogen selectivity due to their ability to dissociate molecular H_2 at the membrane surface [14, 15].

Current research focuses on the fabrication of thin composite metallic-based membranes. Porous materials such as stainless steel (PSS), ceramic, and glass are commonly used as support structures in fabricating these composite membranes [5, 10, 27]. Alumina, a widely used ceramic material, is applied for preparing composite metallic-based membranes because of its distinctive surface properties and good chemical adaptability with metal-based membrane layers [5, 27, 28]. ELP is one of the most common methods for preparing composite metallic-based membranes due to its cost-effectiveness, simplicity, and adaptability to complex geometry support, among other advantages [5, 18, 29, 30].

High permeability and selectivity, good stability (in terms of thermal, mechanical, and chemical), a microstructure free of defects, and a low-cost fabrication technique are key factors in evaluating membrane performance [5]. These parameters can be effectively achieved by using Ni-based membranes [25]. Nickel stands out as a promising material for H_2 separation owing to its excellent catalytic activity [31], high thermal stability [16, 32, 33], cost-effectiveness [16, 25, 32, 34, 35], and strong resistance to deactivation by sulfur-based impurities and carbon monoxide [16, 33]. Over the past few decades, extensive research has focused on developing dense and thin Ni-based composite membranes. However, research [36–41] has highlighted the challenges of depositing a uniform, thin nickel layer (1-2 μm) onto porous supports using the ELP approach. In our recent studies [3, 20, 21], we successfully fabricated dense and defect-free Pd-Ni and Pd-Ag-Ni composite membranes by integrating nickel into pure palladium and Pd-Ag composite membranes through the OIA approach in the ELP technique. These membranes exhibited high hydrogen separation performance while significantly reducing fabrication costs by lowering palladium consumption. However, the feasibility of fabricating a thin, defect-free nickel composite membrane using the OIA process – without the incorporation of palladium – remains insufficiently explored in the current literature. Addressing this gap is essential, as it may enable the development of cost-effective and high-performance hydrogen separation membranes composed entirely of non-precious metals, thereby offering a promising alternative for large-scale industrial applications. This study explores whether such membranes can be effectively fabricated or whether nickel must be incorporated into Pd-based alloys to achieve adequate structural integrity and hydrogen separation performance.

In this study, a thin and uniform nickel layer was created on the homemade modified $\alpha-Al_2O_3$ support by the OIA process. The microstructural characteristics of the membrane, along with the distribution of palladium particle size within the polymer matrix during the activation of the modified support surface, were comprehensively investigated using advanced analytical methods. The gas permeation experiments and H_2 flux mechanism across the membrane were evaluated at different operating conditions using pure H_2 and N_2 gases.

2 Experimental

2.1 Membrane fabrication

The homemade tubular $\alpha-Al_2O_3$ support was fabricated using Al_2O_3 powder (Fibrona Co.) and the gel-casting approach [42, 43]. This support is 60 mm long with an outer diameter of 9 mm and a wall thickness of

3 mm. The support has a porosity of about 40% with an average pores of 0.3 μm [42]. TiO_2 was employed as an intermediate layer to enhance the surface properties of the $\alpha-Al_2O_3$ support by reducing its roughness and pore size [44]. The OIA approach was employed to modify the surface of the $\alpha-Al_2O_3$ support. Building on our earlier studies, the activation process was conducted in two sequential steps [5,45–47]. First, sensitization was achieved by immersing the modified support into a polyethylene glycol (PEG 35000) solution, facilitating Pd particle adhesion in the subsequent activation step. Next, a polyethylene glycol (PEG 6000) solution containing Pd particles was applied to activate the modified $\alpha-Al_2O_3$ support via the dip-coating process. Ultimately, the PEG polymer was thermally decomposed under airflow at approximately 600 °C, leading to the formation of a nanoscale interstice.

The nickel composite membrane was fabricated by sequentially depositing two nickel layers onto the modified support surface through the ELP technique. Each layer required approximately 3-4 hours for plating. The composition of the nickel bath and the experimental conditions employed in this study are provided in Table 1.

Table 1. Ni bath composition and experimental conditions employed in the ELP process.

Component	Concentration (mol/L)
$Ni(OCOCH_3)_2 \cdot 4\,H_2O$	0.12
$Na_2EDTA \cdot H_2O$	0.016
$N_2H_4 \cdot H_2O$ (1 M)	0.4
Lactic acid	0.15
NaOH	0.35
Experimental conditions	
pH	9
T (°C)	80

After each Ni plating step, deionized water at 80 °C was used to rinse the membrane surface. Subsequently, the membrane was dried inside an electrical furnace set to 120 °C for 4 hours, with a controlled temperature ramp of 1 °Cmin^{-1}. Following each plating step, an argon gas leakage test was carried out to inspect the membrane for defects or pinholes. In the last step, the membrane was heated at 700 °C for 24 hours in a hydrogen stream, with a controlled temperature ramp of 0.5 °Cmin^{-1}.

2.2 Membrane characterization

Transmission electron microscopy (TEM, CM-200 FEG Philips microscope) analysis was applied to investigate the distribution of Pd particle size in the polymer solution. Field emission scanning electron microscopy coupled with energy-dispersive X-ray spectroscopy (FESEM-EDS, MIRA3 FEG-SEM, Tescan) was used to characterize the membrane morphology, determine the layer thickness, and analyze the elemental distribution on the membrane surface. X-ray diffraction (XRD, Siemens D500) was employed to analyze the crystalline structure of nickel metal before and after heat treatment. Atomic force microscopy (AFM, Nanosurf Mobile S, Nanosurf Co.) was used to analyze the external surface roughness of the membrane.

2.3 Performance measurement

Gas permeation tests were carried out with a homemade system, illustrated in Figure 1. The tubular nickel composite membrane was sealed at both ends using Viton O-rings, providing an effective membrane area of about 11 cm^2. A tubular membrane module was applied for permeation tests. The mass flow controller (MFC) introduced gas feed onto the external surface of the membrane from the shell side. The permeated gas stream was quantified with a soap-bubble flowmeter for precise flux determination. The shell side pressure was regulated using a back-pressure regulator. Meanwhile, the permeate side was maintained at ambient pressure. Sweep gas was not utilized during the performance assessment. Permeation measurements were conducted using pure H_2 and N_2 gases at temperatures ranging from 25-150 °C and differential pressure of 100-400 kPa.

3 Results and Discussion

3.1 Analysis of membrane characteristics

Figure 2 illustrates the TEM micrograph, revealing the distribution of Pd particle size in the polymer matrix. The Pd particles demonstrated a tight distribution of particle sizes, with an average diameter of approximately 150 nm. Creating a Pd-polymer solution with a tight distribution of Pd particles is crucial for achieving uniform plating and producing a stable, homogeneous membrane layer on the support surface. These results are consistent with the existing literature [20,21,45,46].

Figure 3a shows a FESEM image of the membrane surface before heat treatment at 700 °C in a hydrogen atmosphere. The surface exhibited irregular topography with distinct flower-like structures, possibly attributable to nickel dendritic development in the ELP process. Figures 3b and 3c displays the surface and cross-sectional FESEM images after the heat treatment. A homogeneous nickel layer with small pinholes (highlighted by red circles) and defects were formed after heat treatment (see Figure 3b). The creation of this morphology after heat treatment may be ascribed to the prevention of radial nickel plating and

the localized growth of nickel. This results in forming a thin, dense, and non-homogeneous nickel layer, which is susceptible to structural defects during the heat treatment process. This observation agrees with the existing literature [21, 39]. The membrane had an estimated thickness of around 2 μm. As reported in our previous works [5, 20, 21, 45, 46], a nanoscale space was generated between the membrane layer and the modified $\alpha-Al_2O_3$ support through the OIA technique (see Figure 3c).

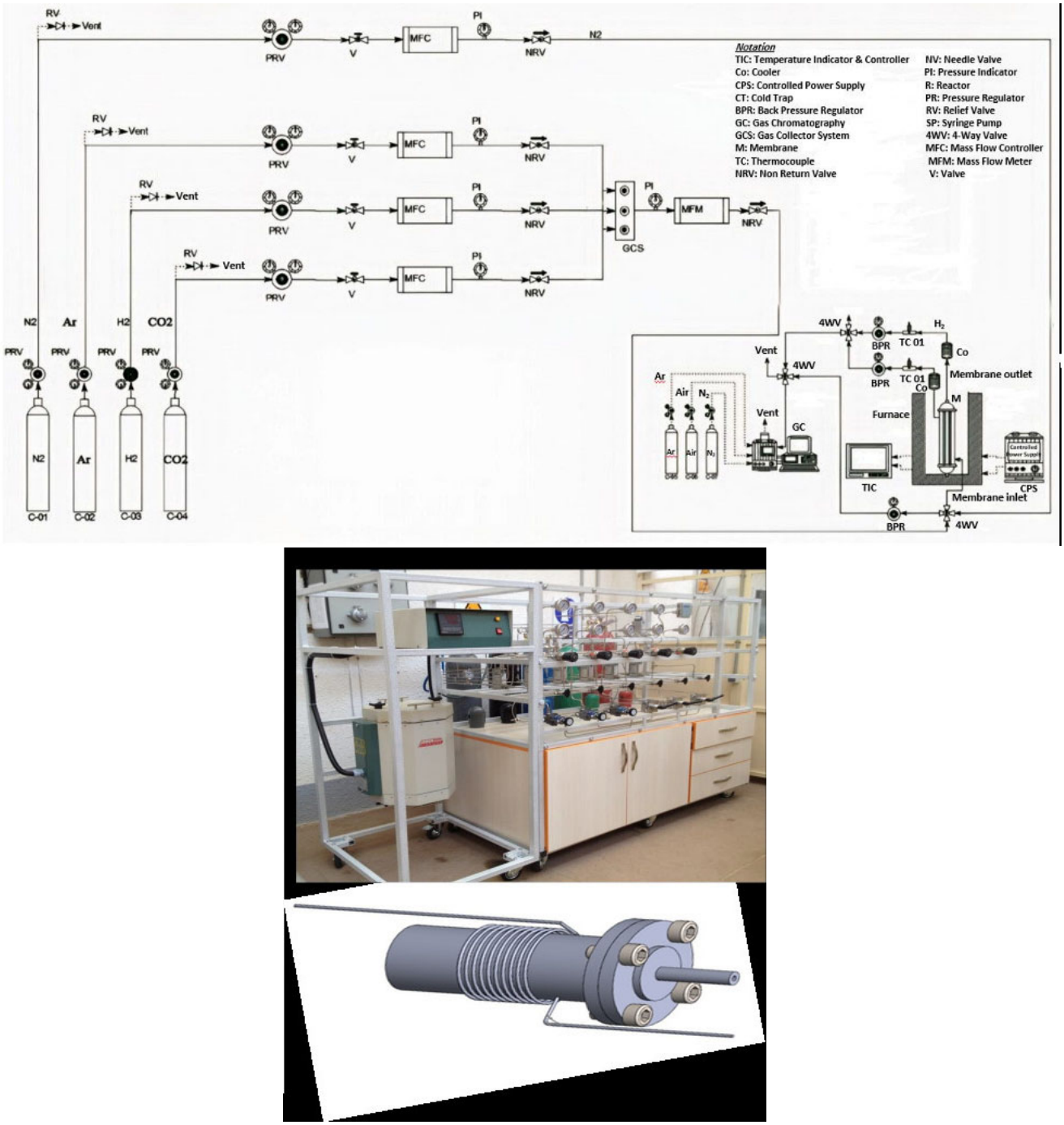

Fig. 1. Schematic illustration of the homemade gas permeation system for gas permeation experiments.

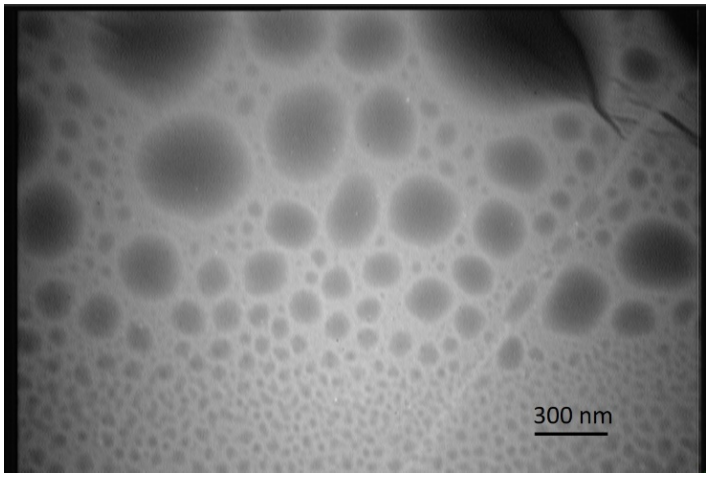

Fig. 2. TEM image of the distribution of Pd particles in the polymer matrix.

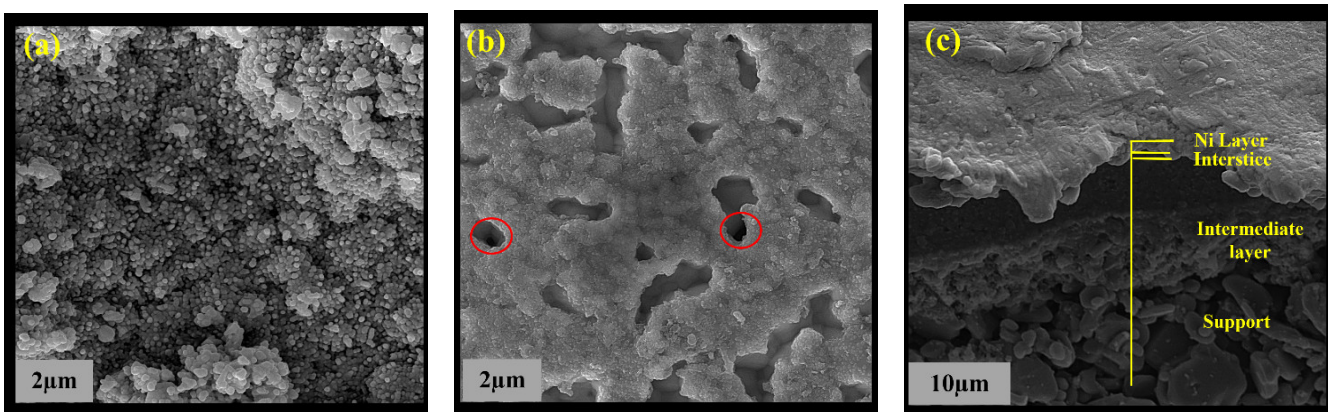

(a) **(b)** **(c)**

Fig. 3. FESEM images of membrane before heat treatment (a) and after heat treatment (b and c).

Figure 4 shows the XRD patterns of the fabricated membrane before and after heat treatment, which reveal changes in its crystalline structure. Before heat treatment, a nickel-rich layer was created on the modified $\alpha-Al_2O_3$ support surface (see Figure 4a). After heat treatment, the XRD pattern revealed additional peaks related to the support. These peaks suggest the creation of some structural defects on the membrane surface, which confirms structural changes caused by the heat treatment (see Figure 4b). These findings are consistent with the existing literature [21,38].

EDS analysis of the membrane surface after heat treatment revealed that the upper layer comprises 99.99% atomic nickel (see Figure 5).

Figure 6 shows an AFM image of the exterior surface of the membrane after heat treatment. The average surface roughness of the membrane was 369 nm, which is higher than the surface roughness reported for Pd-Ni and pure Pd composite membranes in the literature [20,21]. The development of this morphology after heat treatment can be attributed to the prevention of radial nickel plating and localized nickel growth during the ELP process.

Table 2 displays the average roughness factors of the external surface of the fabricated membrane.

Table 2. Surface roughness specifications of the membrane.

Membrane	Roughness factors (nm)			
	S_a	S_q	S_z	S_m
Ni	369	497	1819	199

S_a: the average roughness
S_q: the root average square roughness
S_z: the average distance between the highest peaks and the lowest valleys
S_m: the average distance of profile unevennesses

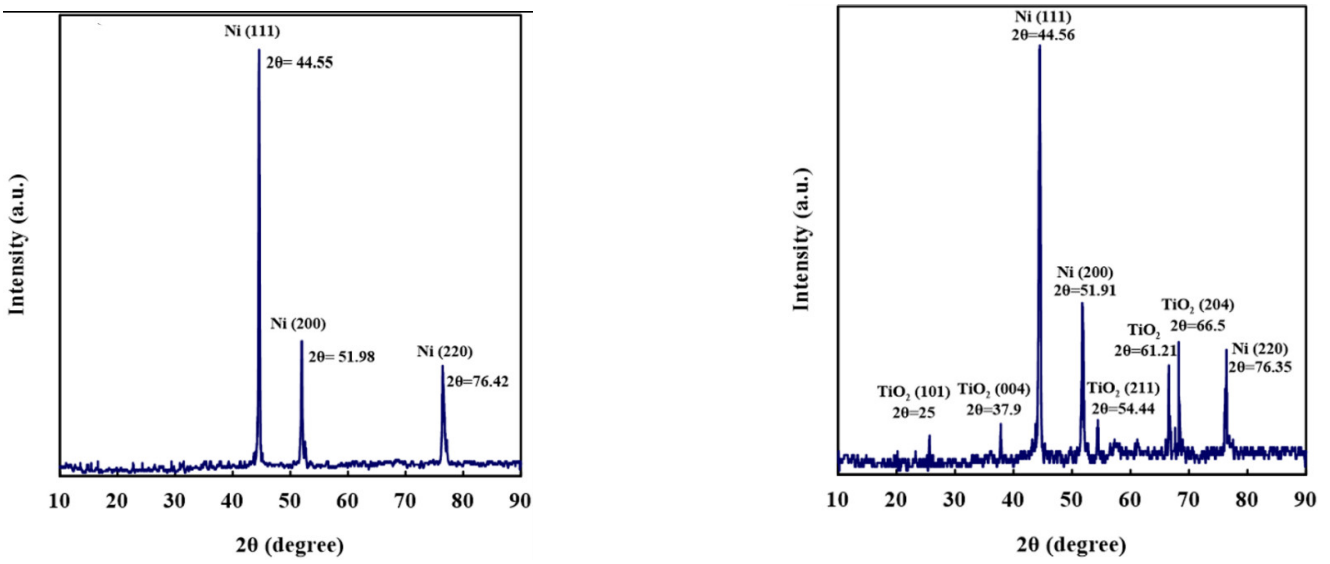

(a) (b)

Fig. 4. XRD patterns of the membrane (a) before and (b) after heat treatment at 700 °C for 24 h under a hydrogen atmosphere.

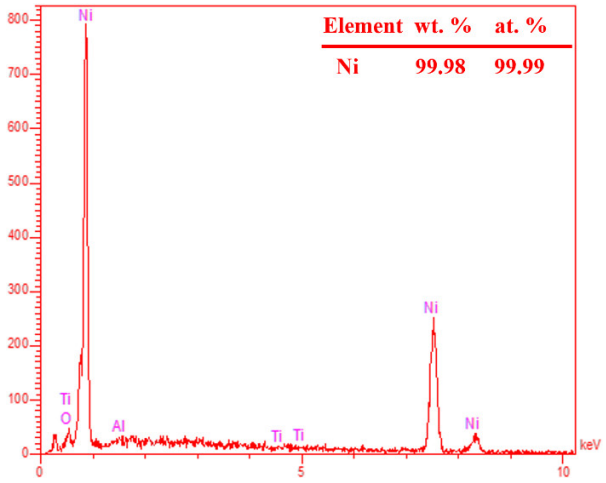

Fig. 5. EDS of the surface of the fabricated membrane after heat treatment at 700 °C for 24 h under a hydrogen atmosphere.

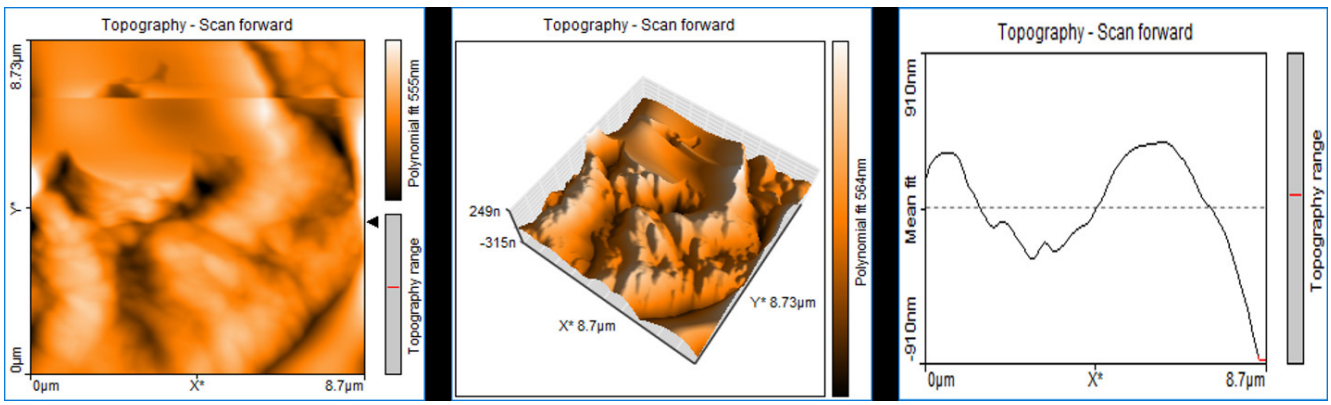

Fig. 6. AFM image of the external surfaces of the membrane after heat treatment at 700 °C for 24 h under a hydrogen atmosphere.

Figure 7 shows the membrane appearance before and after the heat treatment. The membrane surface was black before the heat treatment, but afterward, it changed to a metallic grey color.

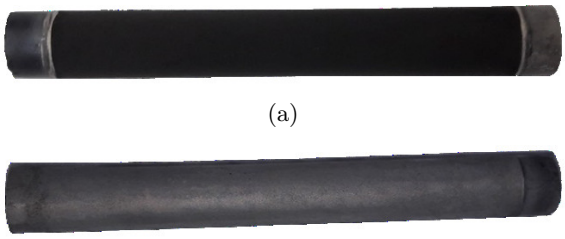

(a)

(b)

Fig. 7. Image of the Ni composite membrane (a) before and (b) after heat treatment at 700 °C **for 24 h under a hydrogen atmosphere.**

3.2 Permeation characteristics of the membrane

After each nickel layer plating, an argon leakage test was carried out on the nickel composite membrane at ambient temperature under different pressure differences (ΔP = 100-300 kPa). The results are shown in Figure 8a. After plating the second nickel layer, some pinholes on the membrane surface were filled with nickel, resulting in almost zero Ar leakage. These results support successfully fabricating a defect-free nickel composite membrane using the OIA method before heat treatment. The Ar leakage across the membrane increased significantly after heat treatment (see Figure 8b). This increase can be attributed to generating some structural defects on the membrane surface in the heat treatment process. These structural changes are probably a result of the prevention of radial nickel plating and localized nickel growth during the ELP process, leading to the cluster sintering of nickel at elevated temperatures. These results are consistent with the existing literature [21,39].

Figure 9 shows the H_2 flux and ideal H_2/N_2 separation factor of the membrane under various pressure differences and temperatures after heat treatment. As shown in Figure 9a, the H_2 flux exhibited a linear increase with rising pressure differences and decreasing temperatures. This observation suggests that Knudsen diffusion was the prevailing mechanism for hydrogen transport through the membrane. Figure 9b illustrates a decrease in an ideal H_2/N_2 separation factor with increasing temperature and pressure differences. The theoretical H_2/N_2 separation factor based on Knudsen diffusion is 3.73, while the experimentally measured separation factor was lower. This decrease is primarily attributed to the contribution of viscous flow in larger pinholes, as well as other potential factors. These results are consistent with the existing literature [21,37,38,48].

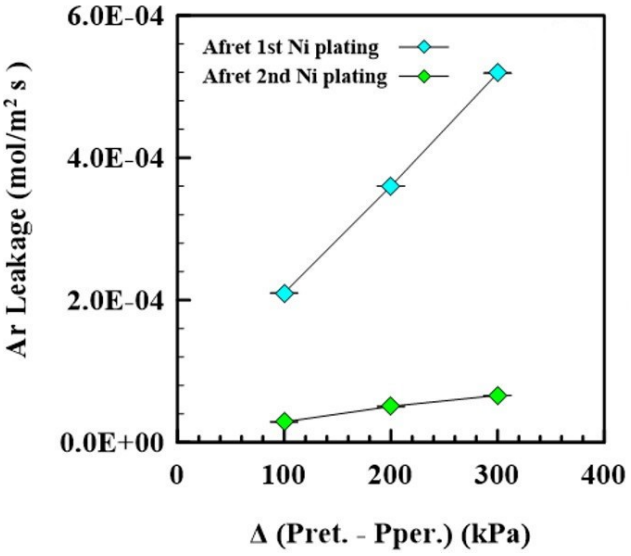

(a)

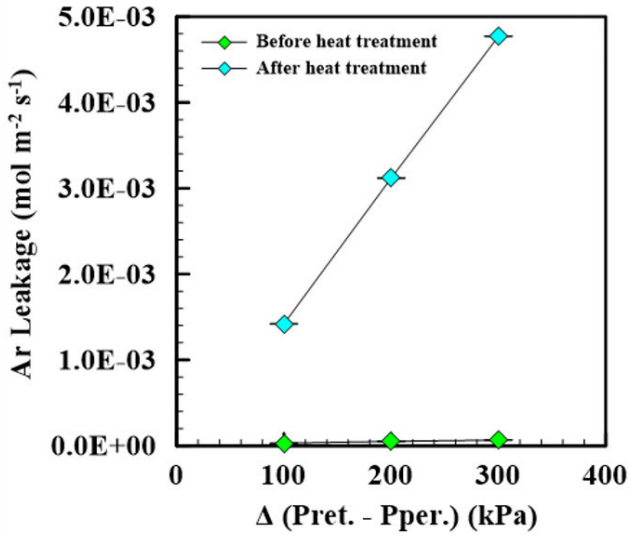

(b)

Fig. 8. Variation of Ar leakage with pressure differences at 25 °C **(a) after each nickel plating and (b) before and after heat treatment of the membrane.**

Table 3 presents a comparative analysis of the performance of the prepared membrane in this study against previously reported studies. Previous investigations have observed higher H_2 permeance, which could be related to preparation conditions that produce membranes with increased permeance but a restricted separation factor (or selectivity).

Table 3. Performance comparison of the membrane developed in this study with reported literature data

Membrane	Method	Thickness (μm)	Temp. (°C)	$P_r - P_p$ (kPa)	H_2 permeance ($molm^{-2}s^{-1}Pa^{-1}$)	H_2/N_2 selectivity	E_a ($kJmol^{-1}$)	Ref.
Ni/Al_2O_3	ELP	1-1.5	25	28	2.61×10^{-7}	3.7	-	[37]
Ni/Al_2O_3	ELP	1-1.5	25	100	2×10^{-7}	3.3	-	[38]
Ni/Al_2O_3	ELP	2	25	100	0.74×10^{-7}	3.32	-	[49]
Ni/Al_2O_3	ELP	2	25	400	0.82×10^{-7}	3	-	This work

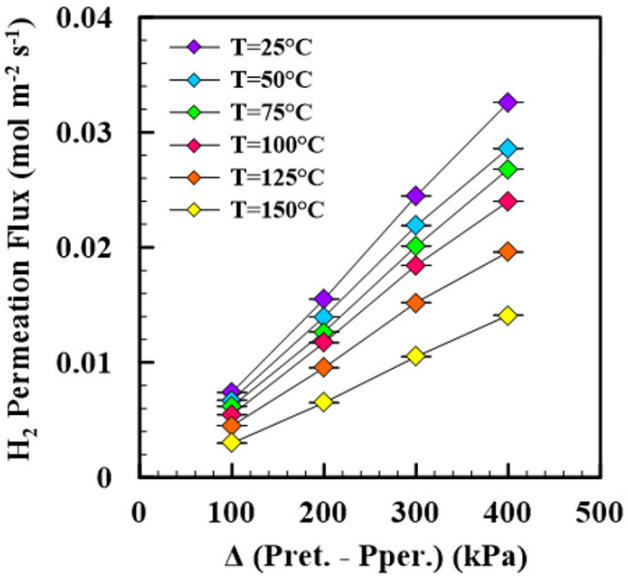

(a)

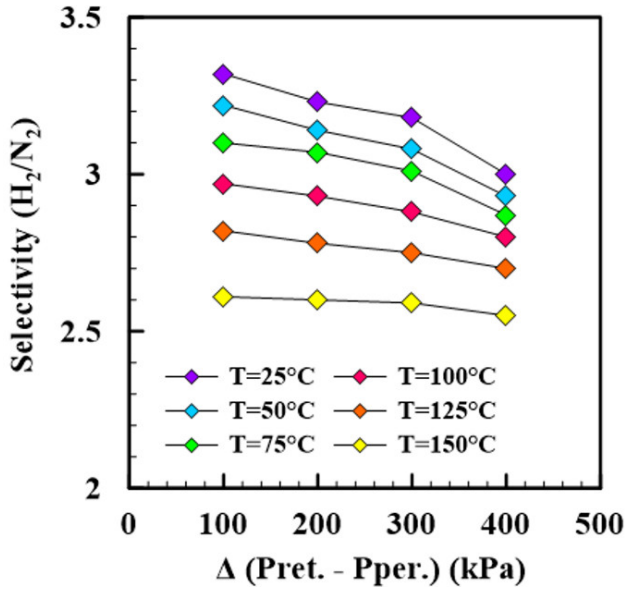

(b)

Fig. 9. (a) Variation hydrogen flux and (b) H_2/N_2 separation factor of the membrane with pressure differences at different temperatures after heat treatment

4 Conclusion

This study presents a novel fabrication method for metal/ceramic membranes, providing an economical substitute for traditional, expensive Pd-based membranes. The main findings are summarized as follows:

- The FESEM image of the membrane surface before heat treatment revealed a dense membrane layer, whereas, after heat treatment, structural defects emerged, which may be attributed to the nickel dendritic development in the ELP process.
- The XRD pattern of the membrane surface after heat treatment revealed support-related peaks and prominent nickel peaks, confirming the structural defects created during the heat treatment process.
- At the temperature of 25 °C and differential pressure of 400 kPa, the H_2 flux of the nickel composite membrane was measured at $3.26 \times 10^{-2}\,\mathrm{mol\,m^{-2}\,s^{-1}}$, with a separation factor of 3 for H_2/N_2. The findings demonstrated that Knudsen diffusion was the prevailing mechanism for hydrogen transport across the membrane.
- While nickel is a promising replacement for Pd-based membranes, fabricating a defect-free and thin ($2\,\mu$m) selective nickel composite membrane remains challenging. To improve performance and reduce fabrication costs, nickel must be incorporated into Pd-based alloys.

Despite the successful demonstration of a cost-effective fabrication method, the fabricated nickel composite membrane exhibited limited hydrogen separation performance, highlighting the need for further improvements in selectivity and long-term stability to enable its practical application in hydrogen purification technologies.

In light of these findings, the developed nickel composite membrane offers a cost-effective alternative for hydrogen purification, particularly in applications where the high cost of palladium membranes is a limitation. Future studies are recommended to optimize the fabrication and heat treatment conditions to minimize defects and enhance membrane performance. Furthermore, the incorporation of alloying strategies could be investigated to further improve membrane performance while maintaining cost-effectiveness, thereby supporting large-scale industrial applications.

Acknowledgments

The authors would like to thank the Nanostructure Materials Research Center (NMRC) and the Department of Chemical Engineering of Sahand University of Technology (SUT) for their invaluable assistance in the preparation of this paper.

References

[1] Kang J, Song Y, Kim T, Kim S. Recent trends in the development of reactor systems for hydrogen production via methanol steam reforming. International Journal of Hydrogen Energy. 2022;47(6):3587-610.

[2] bin Jumah A. A comprehensive review of production, applications, and the path to a sustainable energy future with hydrogen. RSC advances. 2024;14(36):26400-23.

[3] Omidifar M, Babaluo AA. Fabrication of the composite Pd-Ag-Ni membrane by the electroless plating technique for H_2 purification; 2025.

[4] Mobini A, Fassih A, Niknejad S, Zare S. Hydrogen Utilization in Free Piston Engines: A Performance Investigation. Hydrogen, Fuel Cell & Energy Storage. 2025;12(1):31-44.

[5] Omidifar M, Babaluo AA. Hydrogen flux improvement through palladium and its alloy membranes: Investigating influential parameters-A review. Fuel. 2025;379:133038.

[6] Iulianelli A, Brunetti A, Pino L, Italiano C, Ferrante GD, Gensini M, et al. An integrated two stages inorganic membrane-based system to generate and recover decarbonized H_2: an experimental study and performance indexes analysis. Renewable Energy. 2023;210:472-85.

[7] Farzaneh F. Iranian hydrogen production insight: research trends and outlook. Hydrogen, Fuel Cell & Energy Storage. 2021;8(1):23-33.

[8] Bernardo G, Araújo T, da Silva Lopes T, Sousa J, Mendes A. Recent advances in membrane technologies for hydrogen purification. International Journal of Hydrogen Energy. 2020;45(12):7313-38.

[9] Kudapa VK, Mondal S. Hydrogen Membranes: Production, Fabrication, and Applications. CRC Press; 2025.

[10] Cerone N, Zito GD, Florio C, Fabbiano L, Zimbardi F. Recent Advancements in Pd-Based

Membranes for Hydrogen Separation. Energies. 2024;17(16):4095.

[11] Kim TW, Lee EH, Byun S, Seo DW, Hwang HJ, Yoon HC, et al. Highly selective Pd composite membrane on porous metal support for high-purity hydrogen production through effective ammonia decomposition. Energy. 2022;260:125209.

[12] Emhanna SA, Salem RS. Prospects and challenges for the production and use of green hydrogen as a promising energy in Libya. Hydrogen, Fuel Cell & Energy Storage. 2023;11(1):1-7.

[13] Saeedi A, Zangooei F. Impact of product gas recycling on steam methane reforming performance with Ni and Rh catalysts. Hydrogen, Fuel Cell & Energy Storage. 2024;11(3):169-78.

[14] Han Z, Xu K, Liao N, Xue W. Theoretical investigations of permeability and selectivity of Pd-Cu and Pd-Ni membranes for hydrogen separation. International Journal of Hydrogen Energy. 2021;46(46):23715-22.

[15] Zhou Q, Luo S, Zhang M, Liao N. Selective and efficient hydrogen separation of Pd-Au-Ag ternary alloy membrane. International Journal of Hydrogen Energy. 2022;47(26):13054-61.

[16] Dube S, Gorimbo J, Moyo M, Okoye-Chine CG, Liu X. Synthesis and application of Ni-based membranes in hydrogen separation and purification systems: A review. Journal of Environmental Chemical Engineering. 2023;11(1):109194.

[17] Pereira J, Souza R, Oliveira J, Moita A. Hydrogen production, transporting and storage processes – a brief review. Clean Technologies. 2024;6(3):1260-313.

[18] Bosko ML, Dalla Fontana A, Tarditi A, Cornaglia L. Advances in hydrogen selective membranes based on palladium ternary alloys. International Journal of Hydrogen Energy. 2021;46(29):15572-94.

[19] Zhu K, Li X, Zhang Y, Zhao X, Liu Z, Guo J. Tailoring the hydrogen transport properties of highly permeable $Nb_{51}W_5Ti_{23}Ni_{21}$ alloy membrane by Pd substitution. International Journal of Hydrogen Energy. 2022;47(10):6734-44.

[20] Omidifar M, Babaluo AA, Jamshidi S. H_2 permeance and surface characterization of a thin ($2\,\mu$m) Pd-Ni composite membrane prepared by electroless plating. Chemical Engineering Science. 2023;283:119370.

[21] Omidifar M, Babaluo AA. Fabrication of thin ($\sim 2\,\mu$m) pure Ni and Pd–Ni alloy composite membranes by the organic-inorganic activation method for hydrogen separation. International Journal of Hydrogen Energy. 2024;53:1025-36.

[22] Al-Mufachi N, Rees N, Steinberger-Wilkens R. Hydrogen selective membranes: A review of palladium-based dense metal membranes. Renewable and Sustainable Energy Reviews. 2015;47:540-51.

[23] Pal N, Agarwal M, Maheshwari K, Solanki YS. A review on types, fabrication and support material of hydrogen separation membrane. Materials Today: Proceedings. 2020;28:1386-91.

[24] Alizadeh E, Firuzjaei HAVK, Rahimi-Esbo M, Sedighi M. Simulation of integrated purification systems for hydrogen production in methanol steam reforming process. Hydrogen, Fuel Cell & Energy Storage. 2023;10(3):158-99.

[25] Delendik K, Kolyago N, Voitik O. Membranes for ultrapure hydrogen obtaining: nickel versus precious metals. Heat Transfer Research. 2022;53(5).

[26] Ryi SK, Park JS, Hwang KR, Kim DW, An HS. Pd-Cu alloy membrane deposited on alumina modified porous nickel support (PNS) for hydrogen separation at high pressure. Korean Journal of Chemical Engineering. 2012;29(1):59-63.

[27] Kiadehi AD, Taghizadeh M, Rami MD. Preparation of Pd/SAPO-34/PSS composite membranes for hydrogen separation: Effect of crystallization time on the zeolite growth on PSS support. Journal of Industrial and Engineering Chemistry. 2020;81:206-18.

[28] Arratibel A, Medrano JA, Melendez J, Tanaka DAP, van Sint Annaland M, Gallucci F. Attrition-resistant membranes for fluidized-bed membrane reactors: Double-skin membranes. Journal of membrane science. 2018;563:419-26.

[29] Yang Y, Li X, Liang X, Chen R, Guo J, Fu H, et al. Preparation of thin ($\sim 2\mu$m) Pd membranes on ceramic supports with excellent selectivity and attrition resistance. International Journal of Hydrogen Energy. 2023;48(2):662-75.

[30] Tanaka D, Medrano J, Sole J, Gallucci F. Metallic Membranes for Hydrogen Separation. Current Trends and Future Developments on (Bio-) Membranes. Elsevier: Amsterdam, The Netherlands; 2020.

[31] Pişkin F, Öztürk T. Combinatorial screening of Pd-Ag-Ni membranes for hydrogen separation. Journal of Membrane Science. 2017;524:631-6.

[32] Leimert JM, Karl J. Nickel membranes for in-situ hydrogen separation in high-temperature fluidized bed gasification processes. International Journal of Hydrogen Energy. 2016;41(22):9355-66.

[33] Leimert JM, Dillig M, Karl J. Hydrogen production from solid feedstock by using a nickel membrane reformer. Journal of Membrane Science. 2018;548:11-2.

[34] Escalante Y, Tarditi AM. Thermally stable membranes based on PdNiAu systems with high nickel content for hydrogen separation. Journal of Membrane Science. 2023;676:121581.

[35] Zhang H, x Che FHY, j Song Y, Zhou M, Ding D. Effect of annealing treatment on response characteristics of Pd-Ni alloy based hydrogen sensor. Surfaces and Interfaces. 2023;36:102597.

[36] Zhang XL, Xie XF, Huang Y, editors. Pure Ni and Pd-Ni Alloy membranes prepared by electroless plating for hydrogen separation. Trans Tech Publ; 2011.

[37] Haag S EB Burgard M. Pure nickel coating on a mesoporous alumina membrane: preparation by electroless plating and characterization. Surface and Coatings Technology. 2006;201(6):2166-73.

[38] Ernst B, Haag S, Burgard M. Permselectivity of a nickel/ceramic composite membrane at elevated temperatures: A new prospect in hydrogen separation? Journal of membrane science. 2007;288(1–2):208-17.

[39] Changrong X, Xiaoxia G, Fanqing L, Dingkun P, Guangyao M. Preparation of asymmetric Ni/ceramic composite membrane by electroless plating. Colloids and Surfaces A: Physicochemical and Engineering Aspects. 2001;179(2–3):229-35.

[40] Bulasara VK, Thakuria H, Uppaluri R, Purkait MK. Nickel-ceramic composite membranes: Optimization of hydrazine based electroless plating process parameters. Desalination. 2011;275(1–3):243-51.

[41] Bulasara VK, Uppaluri R, Purkait MK. Manufacture of nickel-ceramic composite membranes in agitated electroless plating baths. Materials and Manufacturing Processes. 2011;26(6):862-7.

[42] Babaluo AA, Kokabi M, Manteghian M, Sarraf-Mamoory R. A modified model for alumina membranes formed by gel-casting followed by dip-coating. Journal of the European Ceramic Society. 2004;24(15–16):3779-87.

[43] Ortega F, Valenzuela F, Scuracchio C, Pandolfelli V. Alternative gelling agents for the gelcasting of ceramic foams. Journal of the European Ceramic Society. 2003;23(1):75-80.

[44] Bayati B, Bayat Y, Charchi N, Ejtemaei M, Babaluo A, Haghighi M, et al. Preparation of crack-free nanocomposite ceramic membrane intermediate layers on α-alumina tubular supports. Separation Science and Technology. 2013;48(13):1930-40.

[45] Jamshidi S, Babaluo A. Preparation and evaluation of Pd membrane on supports activated by PEG embedded Pd nanoparticles for ATR membrane reactor. Chemical Engineering and Processing-Process Intensification. 2020;147:107736.

[46] Babalou AA, Jamshidi S. Google Patents, assignee. Palladium composite membrane patent US10882278B;.

[47] Ahmadian NP, Babalou A, Bayati B. Palladium nanoparticles synthesis using polymeric matrix: poly (ethyleneglycol) molecular weight and palladium concentration effects. International Journal Of Nanoscience And Nanotechnology (IJNN). 2007;3(1):37-43.

[48] Ismail AF, Khulbe KC, Matsuura T. Gas separation membranes. Switz Springer. 2015;10:973-8.

[49] Lu H, Zhu L, Wang W, Yang W, Tong J. Pd and Pd-Ni alloy composite membranes fabricated by electroless plating method on capillary $\alpha-Al_2O_3$ substrates. international journal of hydrogen energy. 2015;40(3548):3556.